Journal of Statistical Physics, Vol. 79, Nos. 1/2, 1995

Chaotic Dynamics of High-Order Neural Networks

Ney Lemke,[1] Jeferson J. Arenzon,[1] and Francisco A. Tamarit[2]

Received July 13, 1994; final October 21, 1994

The dynamics of an extremely diluted neural network with high-order synapses acting as corrections to the Hopfield model is investigated. The learning rules for the high-order connections contain mixing of memories, different from all the previous generalizations of the Hopfield model. The dynamics may display fixed points or periodic and chaotic orbits, depending on the weight of the high-order connections ε, the noise level T, and the network load, defined as the ratio between the number of stored patterns and the mean connectivity per neuron, $\alpha = P/C$. As in the related fully connected case, there is an optimal value of the weight ε that improves the storage capacity of the system (the capacity diverges).

KEY WORDS: Neural networks; multineuron interaction; chaotic dynamics.

1. INTRODUCTION

Neural networks have been the subject of intense research in statistical mechanics in the last decade. Besides the equilibrium properties that are reasonably well understood in the framework of spin-glass theory, dynamical properties have attracted much attention: in the limit of low loading or focusing only in the first few time steps, several treatments[1] yielded important results, while only very recently a framework to study fully connected saturated networks was developed by Coolen and Sherrington.[2] There is another limit that can be studied, when the connections are extreme and asymmetrically diluted, and it is interesting mainly for two reasons: the dynamics can be exactly solved (see Derrida, Gardner, and Zippelius,[3] hereafter DGZ) and both dilution and asymmetry are biologically realistic characteristics, absent in the fully connected standard Hopfield model.

[1] Instituto de Física, Universidade Federal do Rio Grande do Sul, C.P. 15051, 91501-970, Porto Alegre, RS, Brazil. E-mail: lemke@if1.ufrgs.br, arenzon@if1.ufrgs.br.

[2] Centro Brasileiro de Pesquisas Físicas, 22290, Rio de Janeiro, RJ, Brazil. E-mail: tamarit@cbpfsu1.cat.cbpf.br.

0022-4715/95/0400-0415$07.50/0

In order to introduce asymmetry in the connections through dilution, the synapses J_{ij} and J_{ji} are cut with probability $1 - C/N$ independently of each other, where C is the mean connectivity of each neuron and the extreme dilution limit is obtained when $C \ll \ln N$ (N is the size of the network). Measuring the network load by $\alpha = P/C$, where P is the number of stored patterns, DGZ found that the diluted version of the Hopfield model is more efficient than the fully connected case ($C = N$)[4]: the critical value above which the system cannot retrieve the stored information is $\alpha_c = 2/\pi$.

Synapses connecting more than two neurons can be considered to both improve the storage capacity of the network[5–13] and to mimic real synapses existing in nervous systems (see refs. 5 and 12 and references therein). Diluted networks with high-order connections were studied in refs. 7–9. Kanter[7] and Tamarit *et al.*[8] considered an energy term like a monomial of order k in the overlap (m_μ^k) and found a discontinuous transition at $\alpha_c(k)$ for $k > 2$. Also, in the (α, T) phase diagram the retrieval phase shrinks as k increases: $\alpha_c(k) \to 0$ as $k \to \infty$, although in this limit the retrieval is perfect. For such models, only fixed points of the dynamics exist. On the other hand, Wang and Ross[9] treated a polynomial, controlling the relative coefficients (weights), and found, besides a retrieval phase, regions where the system can be either periodic or chaotic, depending on the noise or the degree of parallelism in the updating. Although chaotic in the high-dilution limit, when the fully connected model is studied,[12] it does not present any important difference from the standard Hopfield model.

Comparing these results, for some models dilution and asymmetry alone are not sufficient to generate chaotic behavior. Thus, a relevant question is to understand under which conditions the dynamics of the neural network presents other features rather than only fixed points. This is an interesting question because many authors[14] have emphasized the relevance of the chaotic behavior present in natural neural systems like the human brain to the understanding of their striking features such as creativeness, complex interactions among memories, etc. Dynamics comprising only fixed points, although suitable for pattern retrieval, are not adequate in some contexts, since a never-stopping path on the phase space is a characteristic of living brains.

In this paper we study the dynamical effects of introducing a new correction term to the Hopfield model[11, 12] in the extreme dilution limit of both two- and fourth-order synapses with the objective of analyze and highlight their role in the complex dynamics of neural networks. The difference between our model and those studied by Kanter,[7] Tamarit *et al.*[8] and Wang and Ross[9] lies in the nature of the high-order connections we consider. Our model presents an unusual and very puzzling behavior in the

fully connected limit,[12] and this is somehow reflected in the high-dilution case. The paper is organized as follows: Section 2 presents the model, and analytical and numerical results are given for the dynamics in Section 3. In Section 4 we summarize and present the conclusions.

2. THE MODEL

In binary neural networks, such as, for example, the Hopfield model,[15, 16] each neuron is modeled by an Ising variable S_i that can take the values $\{-1, +1\}$ representing the passive and active state, respectively. Possible states of the network are given by N-dimensional vectors $\mathbf{S} \in \{-1, +1\}^N$ and the embedded memories are associated with P of these states, denoted by ξ^μ ($\mu = 1,..., P$).

The fully connected truncated model can be regarded as the Hopfield model with Hebb learning rule plus correction terms and its dynamics is ruled by a Lyapunov function whose long-time behavior (equilibrium states) can be inferred from the statistical mechanics analysis of the system (see refs. 11 and 12 for a detailed study). This system has an extremely rich behavior, different from previously known models, which strongly depends on the value of the weights of the high-order terms.

The dynamics of the extremely diluted and asymmetric version of the truncated model is here studied in two different cases: the initial state has a macroscopic overlap with (a) only one pattern and (b) two correlated patterns (coexisting with $P-2$ uncorrelated ones). Due to the asymmetry in the connections, a Lyapunov function can no longer be defined for the network and hence we are constrained to study the time evolution of the system ruled by the heat bath dynamics, given by

$$S_i(t+1) = \begin{cases} +1 & \text{with probability } \{1+\exp[-2\beta_0 h_i(t)]\}^{-1} \\ -1 & \text{with probability } \{1+\exp[+2\beta_0 h_i(t)]\}^{-1} \end{cases} \tag{1}$$

where the parameter $\beta_0 \equiv T_0^{-1}$ (called the inverse of the temperature) measures the noise level of the net and $h_i(t)$ is the local field acting on the neuron i at time t:

$$h_i = \sum_j J_{ij} S_j - \varepsilon \sum_{j,k,l} J'_{ijkl} S_j S_k S_l \tag{2}$$

The couplings are

$$J_{ij} = C_{ij} \sum_\mu \xi_i^\mu \xi_j^\mu \tag{3}$$

$$J'_{ijkl} = \tfrac{1}{3}(J_{ijkl} + J_{ljki} + J_{kjil}) \tag{4}$$

$$J_{ijkl} = C_{ijkl} \sum_{\mu \neq \nu} \xi_i^\mu \xi_j^\mu \xi_k^\nu \xi_l^\nu \tag{5}$$

and C_{ij} and C_{ijkl} are random variables distributed according to the probabilities ρ and $\tilde{\rho}$:

$$\rho(C_{ij}) = \frac{C}{N}\delta(C_{ij}-1) + \left(1-\frac{C}{N}\right)\delta(C_{ij})$$
$$\tilde{\rho}(C_{ijkl}) = \frac{C}{N^3}\delta(C_{ijkl}-1) + \left(1-\frac{C}{N^3}\right)\delta(C_{ijkl}) \tag{6}$$

where $C \ll \log N$. The asymmetry is introduced through the independence of C_{ij} and C_{ji} (the same holds for C_{ijkl}).

In the fully connected case some of the self-connections are not zero, particularly J_{iikl} and J_{ijkk}. These self-interactions create correlations between the states of neuron i at different times, which apparently prevents one from using the DGZ prescription to obtain the time evolution of the diluted network. Actually, it can be easily shown that in the diluted case the field generated by the self-interactions vanishes in the thermodynamic limit, implying null correlations (because $J_{iikl} \sim J_{kl}P/N$ and $P/N \to 0$ as $N \to \infty$).

3. RESULTS

3.1. One-Pattern Retrieval

Assuming that the updating is parallel and the initial state is correlated with only one of the embedded memories, we are interested in obtaining a recurrent equation,

$$m(t+1) = f(m(t))$$

for the overlap $m(t)$ between the state of the network and this memory,

$$m(t) = \frac{1}{N}\sum_i \langle \xi_i^1 S_i(t) \rangle \tag{7}$$

where $\langle \cdots \rangle$ denotes both thermal and configuration averages. Using standard (and exact) techniques[3] and considering nonbiased patterns, after taking the limit $C \to \infty$ (but slower than $\ln N$), the equation ruling the parallel evolution of the system reads

$$m(t+1) = \int_{-\infty}^{+\infty} \mathcal{D}y \tanh \beta\{m(t) - (2\alpha)^{1/2}\, y[1-\varepsilon m^2(t)]\} \tag{8}$$

where $C\alpha = P - 1$, $\beta = C/T_0$, and $\mathcal{D}y$ is the Gaussian measure:

$$\mathcal{D}y = \frac{dy}{\sqrt{\pi}} e^{-y^2} \tag{9}$$

In the $T = 0$ limit, $f(m)$ becomes

$$f(m) = \operatorname{erf}\left[\frac{m(t)}{(2\alpha)^{1/2}\,[1 - \varepsilon m^2(t)]}\right] \tag{10}$$

and for $0 < \varepsilon < 1$ it is continuous, while it is discontinuous otherwise.

In Fig. 1 we show the fixed points of the equation $m(t+1) = f(m(t))$ as a function of α for several values of $\varepsilon < 1$. For $\varepsilon < 0.266$ the system has only a fixed point that decreases continuously down to 0 at $\alpha_c = 2/\pi$. Above α_c there is only the disordered ($m = 0$) solution. For $0.266 < \varepsilon < 1$ the transition is discontinuous and α_c is greater than $2/\pi$, increasing with ε. In this case there are three different regimes: for $\alpha < 2/\pi$ only the retrieval solutions are stable; for $2/\pi < \alpha < \alpha_c$ this solution coexists with the $m = 0$ one and for $\alpha > \alpha_c$ there is only the disordered solution. In the intermediate regime, an unstable fixed point appears that separates the basins of attraction of the two stable fixed points, and the retrieval basin decreases with α, as can be seen in Fig. 1. Also, for a given value of α, the closer ε is to 1 the better is the retrieval. The retrieval region below α_c, where there exists a nonzero fixed point, is named R_1, while above α_c the disordered phase is named P.

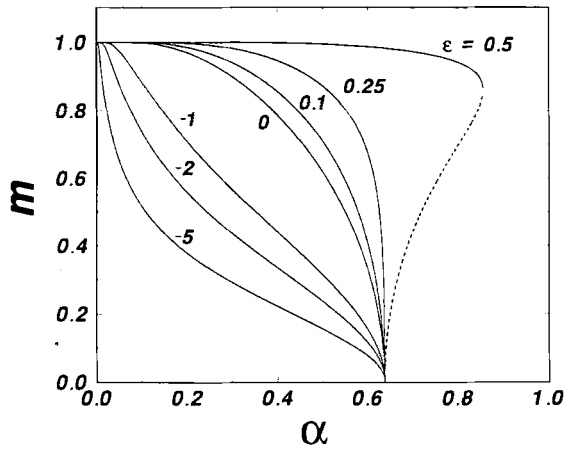

Fig. 1. Fixed points m versus α for several values of ε. The solid line is for stable solutions, while the dashed is for unstable ones. For $\alpha > 2/\pi$ the $m = 0$ solution is always stable.

At $\varepsilon = 1$ there always is the solution $m = 1$ and the unstable fixed point found for $\alpha > 2/\pi$ drops to zero as we approach $\varepsilon = 1$. Hence, the basin of attraction of the retrieval solution increases while the basin of the coexistent disordered solution shrinks to zero when $\varepsilon \to 1$. This means that the network *capacity diverges* and the *retrieval is perfect* for all initial states with nonzero macroscopic overlap! This behavior is the analog of the ε_{opt} found in the fully connected system, where $\varepsilon_{\text{opt}} = (1+\alpha)^{-1}$,[12] while here we have

$$\varepsilon_{\text{opt}} = \frac{1}{1 + P/N} \simeq \frac{1}{1 + \alpha C/N} = 1 \tag{11}$$

since $C \ll \ln N$.

For values of $\varepsilon > 1$ a rich behavior emerges and the system presents a novel kind of retrieval. The overall behavior of the system is presented in Fig. 2, showing several regimes. For a fixed ε and low values of α the system is in a retrieval phase (R_2) where it oscillates between a state with overlap m with the pattern and a state with $-m$ overlap.

As α increases, the system enters a new phase. It starts oscillating between two distinct values of m, say m_1 and m_2 ($|m_1| \neq |m_2|$), while higher periods appear with increasing values of α leading to a chaotic

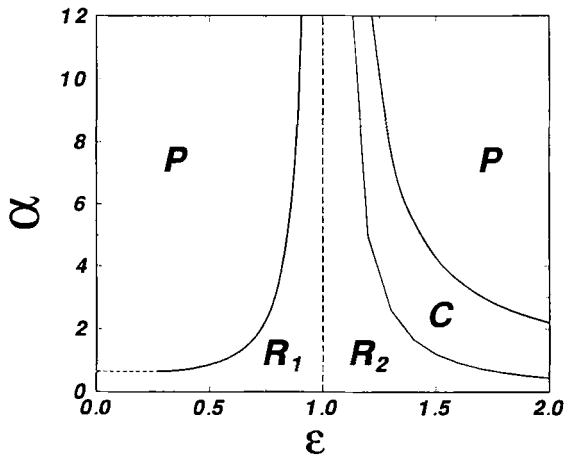

Fig. 2. Phase diagram α versus ε at $T = 0$ for the diluted truncated model. The transition is continuous for $\varepsilon < 0.266$. The optimal value of ε is 1, where $\alpha_c \to \infty$ as $|1 - \varepsilon|^{-2}$. For high values of α the system is in the disordered phase (P) and for $\varepsilon > 1$ it can present a periodic/chaotic phase (C). The retrieval phase may be separated into two, R_1 and R_2, as described in the text.

regime. The route to chaos followed by the system is not exactly period doubling, since it suffers split bifurcations[17]: before doubling the period of the attractor, the system doubles the number of stable attractors. For instance, a period-2 cycle splits into two period-2 cycles before becoming a period-4 cycle. The transition from the twofold attractor to the double-period one occurs when the system enters a superstable orbit (those that contain the critical points). A representative behavior of the system is shown in Fig. 3. The basins of each attractor were also examined and for initial values of m near 0, their domains are extremely mixed.

To decide whether the system evolution is chaotic or not we evaluated the Lyapunov exponent using sequences of $n = 10{,}000$ points. In the aperiodic regime one has $\lambda > 0$, indicating that the system is chaotic, while $\lambda < 0$ if its behavior is periodic. It is worth noting that even in the periodic and in the chaotic attractors, the system always passes very close to the memorized pattern, as can be observed in Fig. 3 for $\varepsilon = 2$. We have verified numerically that for any point in this phase (C), the attractors have at least one point with overlap m near 1, hence it is possible to interpret the cyclic and the chaotic phase as an alternative retrieval phase, in which the system does not recognize a memory by reaching a fixed point, but by wandering around it.

For large enough α the system enters a disordered phase [the only fixed point of Eq. (10)] as can be observed in the phase diagram of Fig. 2 and, as $\varepsilon \to 1$, $\alpha_c \sim |1-\varepsilon|^{-2}$. In the fully connected case there is not a chaotic phase (not even a periodic one), because there the connections are symmetric allowing the introduction of a Lyapunov function.

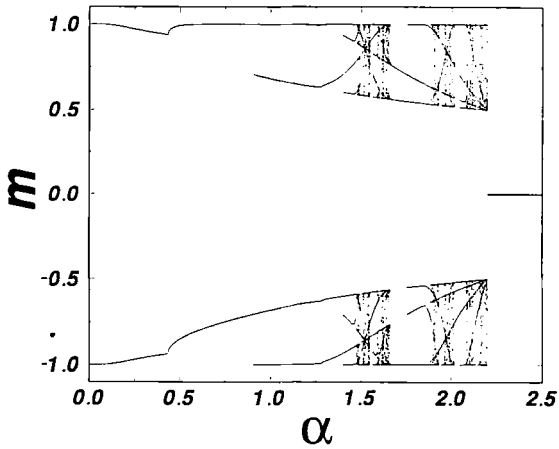

Fig. 3. Plot of m versus α at $T = 0$ for $\varepsilon = 2$. For high values of ε there is only the $m = 0$ solution, while for lower values of ε the system behavior is complex.

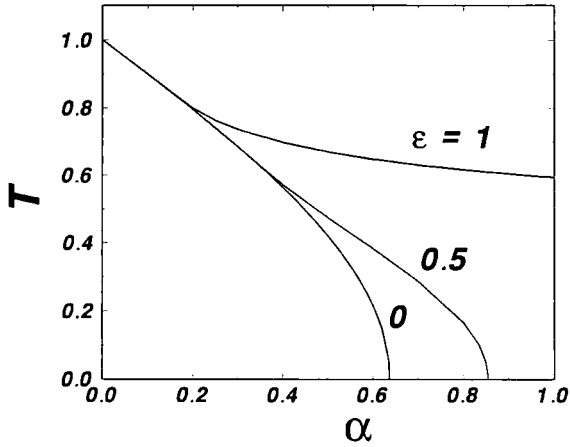

Fig. 4. Phase diagram for some values of $\varepsilon < 1$ showing the critical line T_c separating the only two phases: a retrieval one ($T < T_c$) and the $m = 0$ one ($T > T_c$). For all $\varepsilon < 0.266$ the line T_c is the same as for $\varepsilon = 0$.

Figure 4 displays the T versus α phase diagram for some values of $\varepsilon \leqslant 1$, where there are only fixed-point attractors: one with $m = 0$ (P) and another with $m \neq 0$ (R_1). In particular, for values of ε where the transition is continuous ($\varepsilon < 0.266$) the line T_c is independent of ε and satisfies

$$\beta_c \int_{-\infty}^{+\infty} \mathcal{D}y \operatorname{sech}^2[\beta_c y(2\alpha)^{1/2}] = 1 \tag{12}$$

If $\varepsilon < 1$, the map equation (8) always presents a solution with $m = \pm \varepsilon^{1/2}$ at

$$\beta^* = \frac{\sqrt{\varepsilon}}{2} \ln \frac{\sqrt{\varepsilon} + 1}{\sqrt{\varepsilon} - 1} \tag{13}$$

which means that for $T = T^* = (\beta^*)^{-1}$ the system presents the above solution for all values of α. In the limit $\varepsilon \to 1$, $T^* = 0$ and $m = \pm 1$, as is shown in Fig. 2 and, $\varepsilon \to \infty$, $T^* \to 1$. Figure 5 shows the T versus α phase diagram for $\varepsilon = 2$. Note that, besides the three phases appearing at $T = 0$, we now find also an R_1 phase even for $\varepsilon > 1$. For increasing values of α the $m = 0$ region dominates except for points around T^*. In Fig. 6 the behavior of m for $\varepsilon = 2$ and $\alpha = 2$ is shown as a function of T with the corresponding Lyapunov exponent λ. Note the backward period-doubling bifurcation leading to a retrieval phase for high temperatures: the system leaves the chaotic regime and become periodic as the temperature increases until a certain temperature where it has a fixed point and is able to retrieve the stored information.

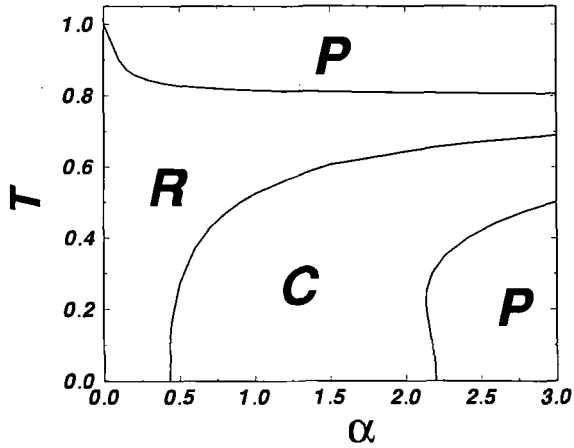

Fig. 5. Phase diagram for $\varepsilon = 2$. The retrieval (R_2) and the periodic or chaotic phases (C) are surrounded by the $m = 0$ one (P). Note that for $T^* \simeq 0.8$ the system has the solution $m = \pm 1/\sqrt{2}$ for all values of α.

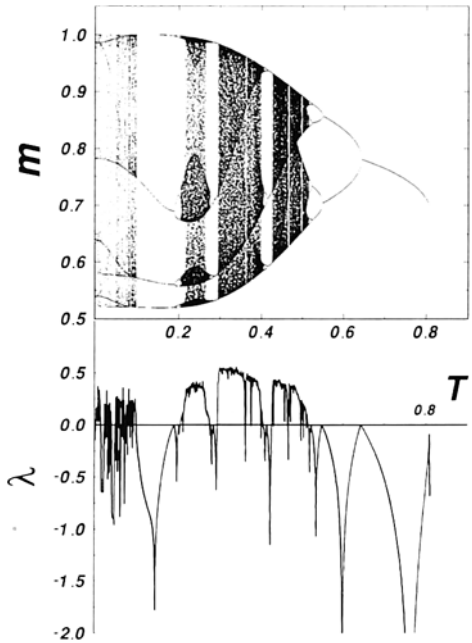

Fig. 6. The overlap m versus T for $\varepsilon = 2$ and $\alpha = 2$ and the corresponding Lyapunov exponent. The system has only a retrieval regime at high temperatures.

3.2. Two-Pattern Retrieval

We also study the case where the initial state has a macroscopic overlap only with the two first memories, which have a fixed macroscopic overlap between them,

$$\kappa = \frac{1}{N} \sum_i \xi_i^1 \xi_i^2 \tag{14}$$

the remaining $P-2$ being uncorrelated. We are interested in determining if the model presents transitions between two or more memories, which may be useful in tasks like retrieving temporal sequences (for a review see ref. 18). These kinds of transitions may be induced here since the fourth-order interactions contain terms that are mixing of all the patterns μ and ν. Another possibility is that instead of oscillating from one pattern top another, a new state is generated that is a combination of the patterns (not only the two involved, but all of them).

The quantities of interest are then the overlaps with these two memories:

$$\begin{aligned} m_1(t) &= \frac{1}{N} \sum_i \langle \xi_i^1 S_i(t) \rangle \\ m_2(t) &= \frac{1}{N} \sum_i \langle \xi_i^2 S_i(t) \rangle \end{aligned} \tag{15}$$

and the time evolution equations for them are ruled by

$$\begin{aligned} M(t+1) &= (1+\kappa) \int \mathscr{D}y \tanh \beta \left[M \left(1 - \varepsilon \frac{M^2 - m^2}{4} \right) \right. \\ &\quad \left. - y(2\alpha)^{1/2} \left(1 - \frac{\varepsilon(M^2+m^2)}{2} \right) \right] \\ m(t+1) &= (1-\kappa) \int \mathscr{D}y \tanh \beta \left[M \left(1 + \varepsilon \frac{M^2 - m^2}{4} \right) \right. \\ &\quad \left. - y(2\alpha)^{1/2} \left(1 - \frac{\varepsilon(M^2+m^2)}{2} \right) \right] \end{aligned} \tag{16}$$

where

$$M = m_1 + m_2, \qquad m = m_1 - m_2 \tag{17}$$

The attractors of these equations were numerically studied starting always from the initial condition $m_1(0)=1$ and $m_2(0)=\kappa$ in the cases $\alpha=0$ and $T=0$. Five different phases were distinguished: a retrieval one (R_1) which corresponds to a fixed point with $|m_1|>|m_2|>0$, another retrieval phase (R_2) in which the system oscillates in a period-two cycle between the states with $|m_i|=\text{cte}$, $|m_1|>|m_2|$, a mixed phase (M) with $m_1=m_2\neq 0$, a disordered phase (P) with $m_1=m_2=0$, and a cyclic/chaotic one (C).

In the preceding section when one considered macroscopic overlap with only one pattern, the DGZ equation was recovered when $\alpha=0$. In the same limit, but when the system has macroscopic overlap with two memories, the DGZ equations are no longer recovered: there is still an ε dependence on the equations, even when $\kappa=0$. In other words, the system may present cyclic and chaotic regimes, absent if one looks for a retrieval solution. Surprisingly, the system may behave chaotically even when all sources of noise are absent.

In Fig. 7 we present the phase diagram T versus ε for $\kappa=0.2$ and $\alpha=0$. For $T=0$ the system present only two phases: the retrieval one for $|\varepsilon|<\kappa^{-1}$ and the cyclic/chaotic one for $|\varepsilon|>\kappa^{-1}$, while the mixed phase appears for a given temperature that depends on the value of κ. It is important to stress that the boundary between the retrieval phase and the cyclic/chaotic one for positive ε shows the first appearance of cyclic orbits: inside the C phase there are islands of retrieval. Also, in the boundary between the mixed phase and the disordered one there is a point ε^* above which the transition is continuous and below which it is discontinuous. It

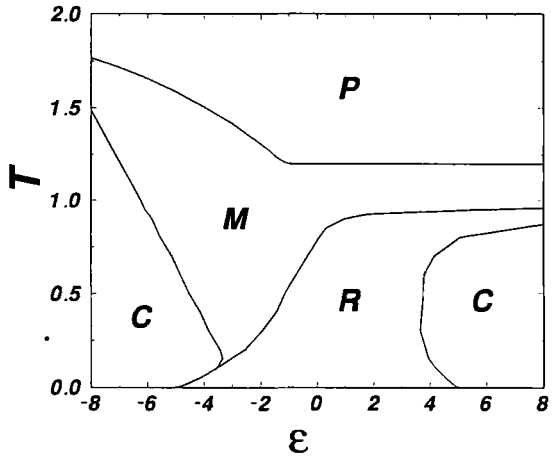

Fig. 7. Phase diagram for $\alpha=0$ and $\kappa=0.2$ in the case where there is macroscopic overlap with two memories (see text).

can be shown that the transition line in the continuous case is given by $T_c = 1 + \kappa$.

In the case $\alpha \neq 0$ and $T = 0$, the α versus ε phase diagram is qualitatively similar to the one in Fig. 2, except for the appearance of the mixed phase. There is also an optimal value for ε where the capacity diverges, given by $\varepsilon_{\text{opt}} = 1 - \kappa^2$, and the boundary between the disordered phase and the mixed one is $\alpha_c = 2(1 + \kappa)^2/\pi$.

4. CONCLUSIONS

We presented an exact solution for the dynamics of a model for neural networks with high-order interactions that shows a very rich behavior depending on the parameters α, ε, and T. In analogy with the related fully connected model, there is an optimal value of ε for which the model always retrieves the embedded information. It is important to stress that for some values of ε the retrieval region is found at high values of T: amazingly, as the temperature is decreased, the system passes from a disordered phase to an ordered one and, after passing through a region where it presents cyclic and chaotic orbits, it reenters the paramagnetic region. In this case, the presence of thermal noise may improve the retrieval abilities of the system.

The periodic and chaotic behaviors are not present for $\varepsilon < 1$ because in this case the one-dimensional map equation (8) is invertible and continuous, not allowing chaos.[19] Physically, the reason for this is that above $\varepsilon = 1$ the Hopfield second-order term is surpassed by the fourth-order one and, due to the mixing of patterns on the synapses (the presence of both μ and ν in the learning rule), cycles are introduced. The absence of this kind of transition in the fully connected model is due to the possibility of symmetrization of all the connections and hence a Lyapunov function exists implying the existence of fixed points only. This is analogous to some models where the task is to retrieve temporal sequences[18] and the learning rule contains pointers explicitly storing the transitions between states.

In the case of macroscopic overlap with two patterns a new phase that mixes these two memories appears. Its presence is an indication that the study of the generalization abilities of the model may reveal some interesting features. Another fact is that at $\alpha = 0$, the one-pattern dynamics recovers the DGZ equation, while in the two-pattern case, even when the two patterns are totally independent ($\kappa = 0$), the dynamics still depends on ε. Also, in the noise-free situation (both $\alpha = 0$ and $T = 0$) the system presents cycles and chaos.

Comparing these results with the ones obtained in the study of the dynamics of the generalized Hopfield model,[9] some points deserve to be stressed. First of all, the equation describing their dynamics is always

continuous. Second, in their model there is no periodic/chaotic behavior if the noise level is set too low. This is because the nonmixing memories nature of the connections.

Due to the very complex nature of the system behavior, it would also be interesting to study the thermodynamics of the symmetric diluted case[20] trying to see the interplay between the fully connected case and the highly diluted one.

ACKNOWLEDGMENTS

We acknowledge R. M. C. de Almeida for several interesting discussions and for encouraging this work. We are also indebted to M. C. Barbosa, J. C. M. Mombach, F. B. Rizatto, D. Stariolo, and C. Tsallis for useful discussions. F. A. T. acknowledges the kind hospitality of the IF-UFRGS during his stay at Porto Alegre. This work was partially supported by Brazilian agencies CNPq, FINEP, and FAPERGS.

REFERENCES

1. A. C. C. Coolen and Th. W. Ruijgrok, *Phys. Rev. A* **38**:4253 (1988); T. B. Kepler and L. F. Abbott, *J. Phys.* (Paris) **49**:1657 (1988); E. Gardner, B. Derrida, and P. Mottishaw, *J. Phys.* (Paris) **48**:741 (1987).
2. A. C. C. Coolen and D. Sherrington, *Phys. Rev. Lett.* **71**:3886 (1993); A. C. C. Coolen and D. Sherrington, *Phys. Rev. E* **49**:1921 (1994).
3. B. Derrida, E. Gardner, and A. Zippelius, *Europhys. Lett.* **4**:167 (1987).
4. D. J. Amit, H. Gutfreund, and H. Sompolinsky, *Ann. Phys.* (NY) **173**:30 (1987).
5. P. Peretto and J. J. Niez, *Biol. Cybern.* **54**:53 (1986).
6. E. Gardner, *J. Phys. A* **20**:3453 (1987); L. F. Abbott and Y. Arian, *Phys. Rev. A* **36**:5091 (1987); D. Horn and M. Usher, *J. Phys.* (Paris) **49**:389 (1988).
7. I. Kanter, *Phys. Rev. A* **38**:5972 (1988).
8. F. A. Tamarit, D. A. Stariolo, and E. M. F. Curado, *Phys. Rev. A* **43**:7083 (1991).
9. L. Wang and J. Ross, *Phys. Rev. A* **44**:R2259 (1991).
10. R. M. C. de Almeida and J. R. Iglesias, *Phys. Lett. A* **146**:239 (1990); J. J. Arenzon, R. M. C. de Almeida, and J. R. Iglesias, *J. Stat. Phys.* **69**:385 (1992).
11. J. J. Arenzon, R. M. C. de Almeida, J. R. Iglesias, T. J. P. Penna, and P. M. C. de Oliveira, *Physica A* **197**:1 (1993).
12. J. J. Arenzon and R. M. C. de Almeida, *Phys. Rev. E* **48**:4060 (1993).
13. D. Bollé, J. Huyghebaert, and G. M. Shim, *J. Phys. A* **27**:5871 (1994).
14. C. A. Skarda and W. J. Freeman, *Behav. Brain Sci.* **10**:161 (1987).
15. J. J. Hopfield, *Proc. Natl. Acad. Sci. USA* **79**:2554 (1982).
16. J. Hertz, A. Krogh, and R. G. Palmer, *Introduction to the Theory of Neural Computation* (Addison-Wesley, Reading, Massachusetts, 1991).
17. J. Testa and G. A. Held, *Phys. Rev. A* **28**:3085 (1983).
18. R. Kuhn and J. L. van Hemmen, In *Physics of Neural Networks*, E. Domany, J. L. van Hemmen, and K. Schulten, eds. (Springer, 1990).
19. E. Ott, *Chaos in Dynamical Systems* (Cambridge University Press, Cambridge, 1993).
20. A. Canning and E. Gardner, *J. Phys. A* **21**:3275 (1988).